Characteristics of Lead and Sulfur Plasma Parameters by Optical Emission Spectroscopy

Marwa J. Ketan, Kadhim A. Aadim*

Department of physics, College of Science, University of Baghdad, Baghdad, Iraq

Abstract

This study uses the optical emission spectroscopy (OES) technique to find the lead(Pb) and sulfur (S) plasma parameters employing a pulse of Nd: YAG laser (Q-switched 1064nm wavelength) and different laser energies of (400,500,600 and 700 mJ). The electron temperature T_e (eV) is calculated using the Boltzmann-Plot method, and the electron density n_e (cm^{-3})is determined by the Stark broadened way. Moreover, Debye length λ_D (cm) and plasma frequency ω_p (Hz) are studied as a function of laser energy. An apparent increase was noted in the electron temperature of lead plasma and a decrease in sulfur plasma. The results also showed that each increase in the laser intensity causes an increase in the optical emission peaks. This experiment was carried out under atmospheric pressure.

Keywords: Laser-induced breakdown spectroscopy (LIBS), Nd:YAG Laser, Optical Emission Spectrometer, Pb Plasma, S plasma.

خصائص معلمات بلازما الرصاص والكبريت بواسطة التحليل الطيفي للانبعاث الضوئي

مروة جاسم كيطان , كاظم عبدالواحد عادم*

قسم الفيزياء, جامعة بغداد, بغداد, العراق

الخلاصة

في هذه الدراسة تم استخدام تقنية التحليل الطيفي للانبعاث الضوئي (OES) للعثور على معلمات بلازما الرصاص والكبريت باستخدام ليزر النيديميوم ياك ذو الطول الموجي 1064nmوبطاقات ليزر (400,500,600 and 700 mJ). تم حساب درجة حرارة الالكترون باستخدام طريقة بولتزمان وكثافة الالكترون بطريقة توسيع ستارك وطول ديباي وتردد البلازما كدوال لطاقة الليزر.حيث اظهرت النتائج زيادة واضحة في درجة حرارة الالكترون للرصاص وانخفاض في الكبريت كما اظهرت ايضا ان كل زيادة في شدة الليزر تسبب زيادة في قمم الانبعاث الضوئية .وتم اجراء هذه التجربة تحت الضغط الجوي.

1. Introduction

Recently, laser-induced breakdown spectroscopy (LIBS) has become a versatile and one of the standard techniques for plasma diagnosis[1]. . The importance of this technique lies in the preliminary analysis of materials (liquid, solid and gaseous), and it can provide

---

*Email: kadhim_adem@scbaghdad.edu.iq

information about the chemical composition of the sample. Because of this, a lot of different applications can be used [2]which include thin-film deposition, material identification, and engineering and environmental monitoring. Understanding the physical phenomena that take place inside a pulsating plasma, as well as developing new analytical methods, is a major focus of many scientists and researchers. This technique provides analysis of materials in solids, gases and liquids in a short period of time, with high accuracy [3]. Plasma is produced by laser pulses focused on a sample, where a sharp temperature change occurs to overcome the bonding forces between its nuclei and its electron. The emission spectra produced in most cases are of different types, ranging from ultraviolet to visible and infrared. The resulting plasma spectrum is collected by a optic-fibre cable[4]. The plasma formed in this way contains ions and atoms in various excited states, emitting radiation during the transition to the lower energy levels which is received by a optic-fibre cable. In plasma diagnosis electron density, electron temperature, Debye length, and plasma frequency are measured. Plasma properties are affected by many different factors such as chemical properties of target , laser wavelength, number of pulses, energy, pulse duration, and atmosphere in which the process takes place [5]. The elements lead and sulfur has been used in this research to produce the plasma. Lead is known as a dangerous and toxic metal. It is found in a variety of different materials, such as food, paint plastic toys, and geological samples [6]. Sulfur is known to have very high ionization energy, so obtaining emission spectra in laser-induced breakdown spectroscopy is a problem; in addition, there are few spectral emissions in the sulfur atom that are suitable to be measured and detected. The best emission lines occur in the ultraviolet region[7]. The main objective of this article is to find the plasma parameters of the elements lead and sulfur in air at atmospheric pressure.

2. Experimental Setup

A Q-switched Nd: YAG laser-produced the plasma laser with a wavelength of 1064 nm and a frequency of 6 Hz, with different laser energies of (400, 500, 600 and 700 mJ). Samples of sulfur and lead were used. These samples, which served as the targets, were pressed, under a pressure of 70 MPa with a hydraulic press for 10 minutes, into the shape of circular disks each with a diameter of 1 cm. This experiment was carried out in atmospheric air, where a laser beam was focused on the target. An optical emission spectrometer captured the light plasma emissions by placing a fibre-optic cable at a distance of 1cm from the target, as shown in Figure 1.The emission results for the spectrum were compared with the NIST data base.
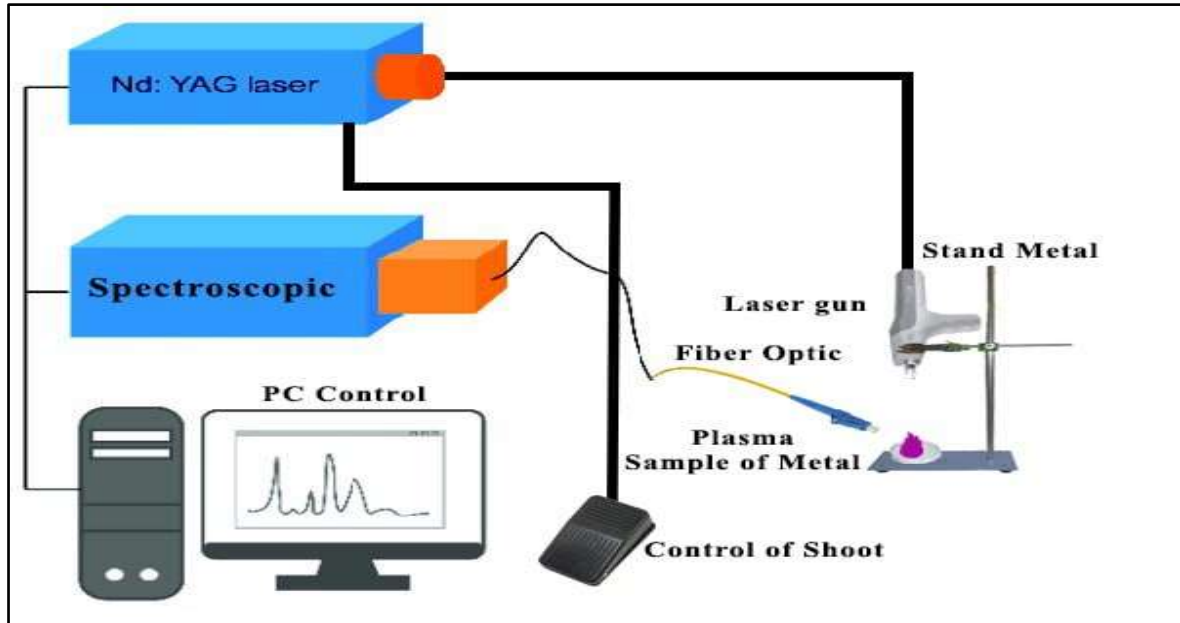
Figure 1: Laser-Induced Breakdown Spectroscopy (LIBS) System Configuration

3. Results and Discussions

3.1 Plasma Emission Studies:

3.1.1 Sulfur Plasma

The emission spectrum of sulfur plasma at different laser energies in the atmosphere ranging from 250 nm to 1100 nm was recorded, as shown in Figure 2. Many emission peaks can be noticed, including the neutral emissions S (I), which are four spectral lines at 450, 745, 922.8, and 1063 nm., and the ionic emissions S (II) of eight spectral lines at 368, 393.9, 414.3, 483.5, 521.2, 546.7, 652.1 and 825.8 nm. As the laser energy increased, the intensity of the peaks increased. This is due to the increase in the removed electrons during the ionization process of the element and the increase in the rate of production of ions and atoms[8].
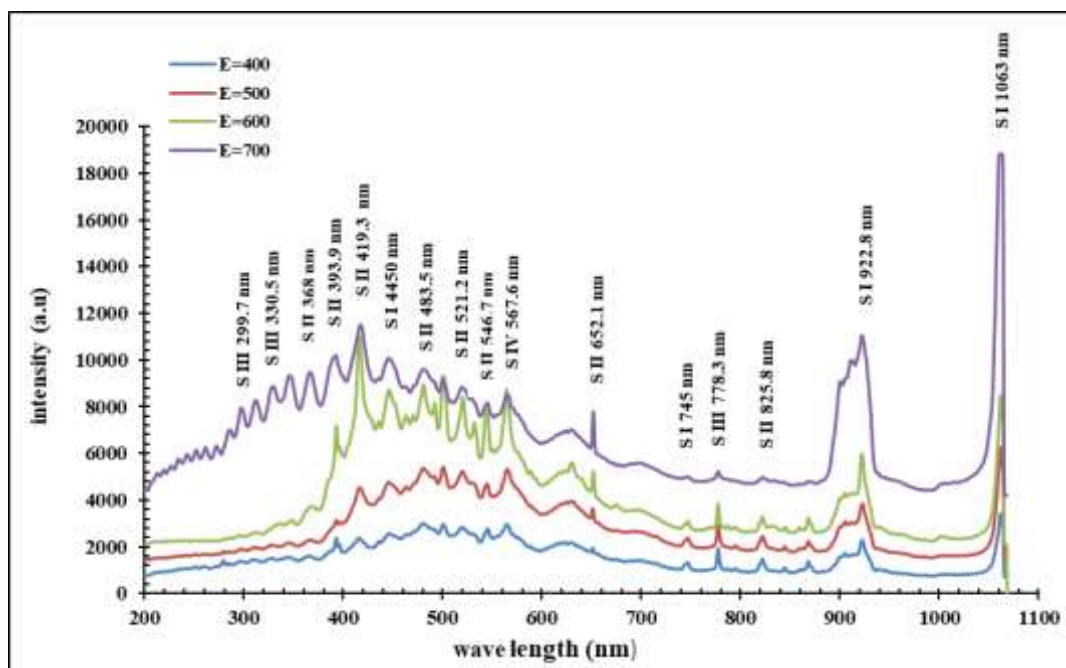

Figure 2: Emission spectrum of predominantly neutral and ionized sulfur plasma generated by the 1064 nm laser in region 200–1100 nm.

3.1.2 Lead Plasma

The emission spectrum of lead plasma in the atmosphere ranging from 200 nm to 570 nm was recorded, as shown in Figure 3. Many spectral emissions can be noted, including the ionizing Pb (II), which has four spectral lines at 220.3, 424.4, 438.6, and 560.8 nm and the neutral emissions Pb(I), which have eight spectral lines at 223.9, 261.4, 280.1, 357.2, 368.3, 373.9, 405.7 and 500.6 nm, which are more than the ionized spectral lines. Through the recombination process, the electrons emitted during the ionization process are recombine [9].
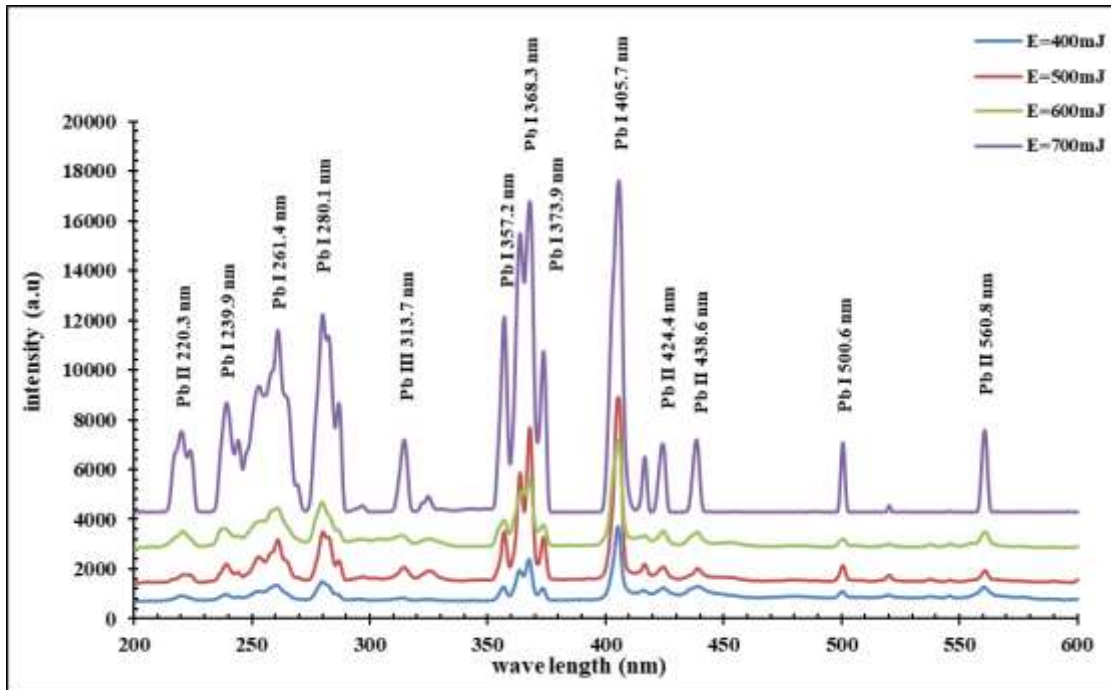

Figure 3: Emission spectrum of predominantly neutral and ionized lead plasma generated by the 1064 nm laser covering the region 150–650 nm

3.2 Determination of the Electron Temperature

The spectral emissions of lead (Pb) and sulfur (S) plasma are essential for calculating the plasma parameters, including the electron temperature. Understanding the plasma ionization, disintegration, and excitation processes can aid in determining the plasma temperature. Material irritated by an intense laser beam loses many electrons from its outermost atoms as those bonds are broken, resulting in evaporation. The temperature is found using Boltzmann plot employing the following equation[10]:

$$\mathrm{Ln}\left[\frac{I_{ki}\lambda_{ki}}{A_{ki}g_{ki}}\right]=ln\left[\frac{N(T)}{U(T)}\right]-\frac{E_k}{k_BT} \qquad \ldots\ldots\ldots\ldots \ (1)$$

Where: λ_{ki} is the transition wavelength, I_{ki} is the integrated line intensity of the transition involving a lower level (i) and upper level (k), g_k is the statistical weight of level (k), A_{ki} is the transition probability, $U(T)$ is the partition function, $N(T)$ is the total number density, E_k is the energy of the upper level, T is the electron temperature, and k_B is Boltzmann constant. A plot of ln (I_λ/Ag) versus the energy E_k gives a straight line with a slope equal to ($-1/k_BT$) as shown in Figure 4 and Figure 5 . With the lead target, electron temperature varied with energy, as shown in Table 1 and Figure 6. Electron temperature increased from 0.48eV to 0.58eV as the laser energy increased from 400mJ to 700mJ. This temperature increase is due to the laser beam absorbing from electrons. These results agree with those of Hanif et al. [11]. As for the element sulfur, the temperature values of (0.44 - 0.40 eV) decreased with the energy values (400 - 700 mJ), as shown in Table 1 and Figure 7. This decrease in temperature

is due to the rapid transformation of thermal energy into kinetic energy when the plasma expands. These results are in agreement with those of Hanif et al.[12].
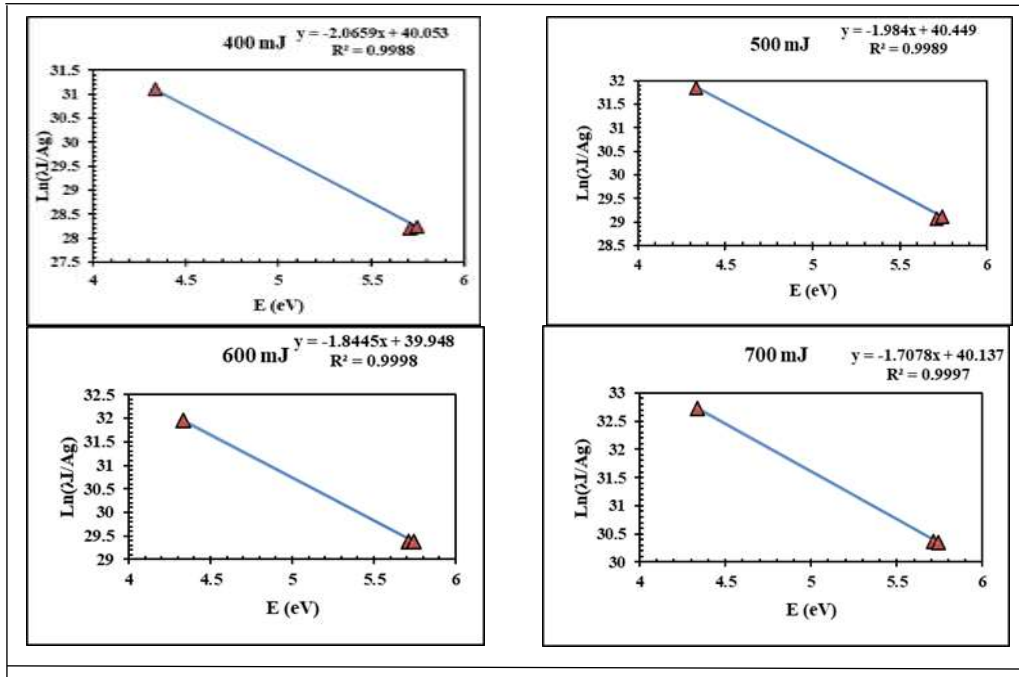

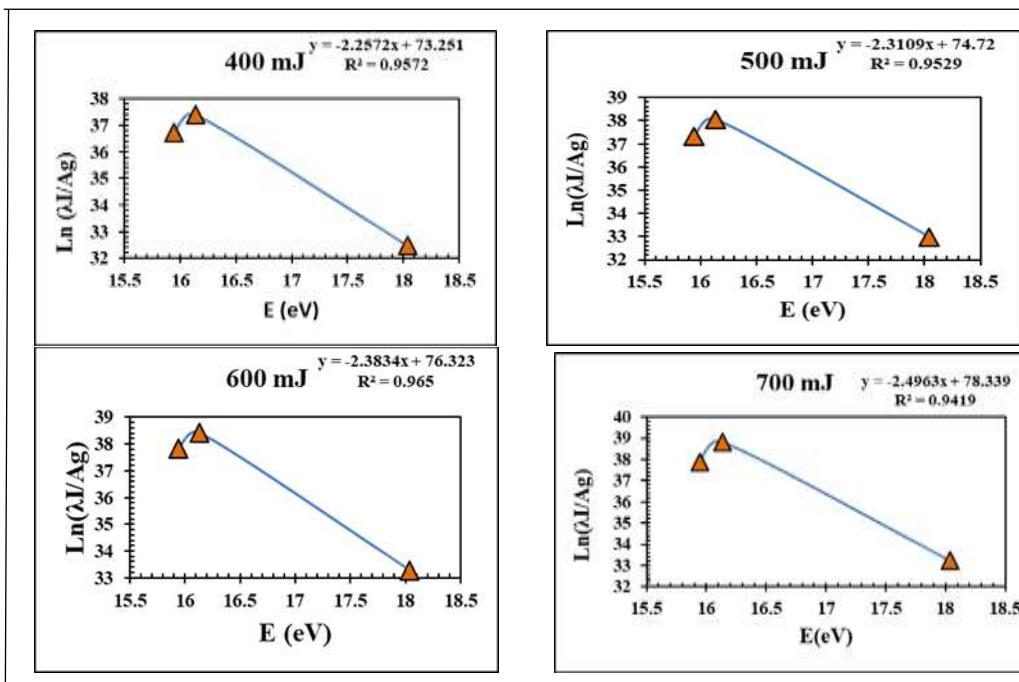**Figure 4:** The Boltzmann plot for lead Pb in (400, 500, 600, 700mJ)

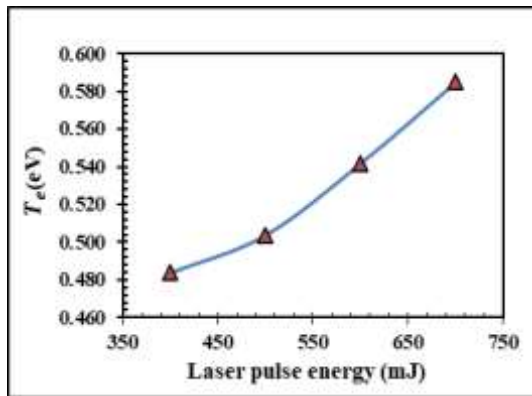**Figure 5:** The Boltzmann plot for sulfur S in (400, 500, 600, 700mJ)

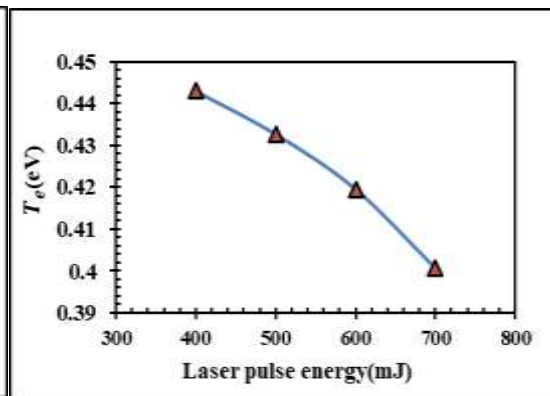**Figure 6:** Electron Temperature of the Pb Plasma

Figure 7: Electron Temperature of the S Plasma

3.3 Determination of Electron Number Density

Measuring Stark broadening is one of the most reliable processes for determining the electron density, calculated for the width of one line of an ion or one atom. This broadening occurs due to the collision of charged particles with the emitted atoms. The electron density can be calculated according to the following relation [13]:

$$n_e = \left(\frac{\lambda_{FWHM}}{2\omega}\right) \times 10^{16} \qquad \ldots\ldots\ldots (2)$$

where n_e is the electron density (cm^{-3}), ω is the electron impact parameter and λ_{FWHM} refers to the Stark full-width at half-maximum. In both elements, lead (Pb) and sulfur (S), the electron density values increased with the increase of laser energy. This is due to the absorption of laser photons in plasma by electron-neutral inverse Bremsstrahlung and the fact that Stark broadening increases with the increase of the laser intensity. As the laser energy changed between (400-700 mJ), the n_e values for lead ranged between (1.65×10^{18} -2.4×10^{18} cm^{-3}), and the values for sulfur ranged between (1.5×10^{18}-2.4×10^{18} cm^{-3}) as shown in Figures 8 for Pb and 9 for S and Table 1.These results agree with those of Sanghapi et al.[2] and Hanif et al.[12].

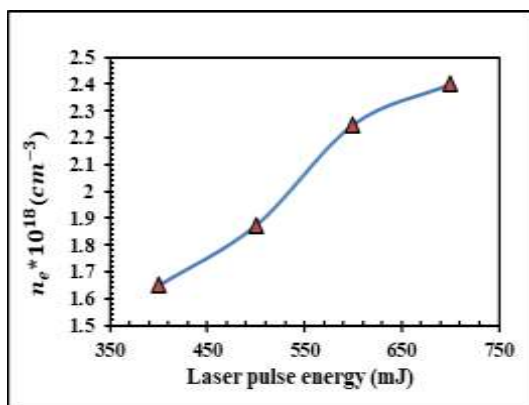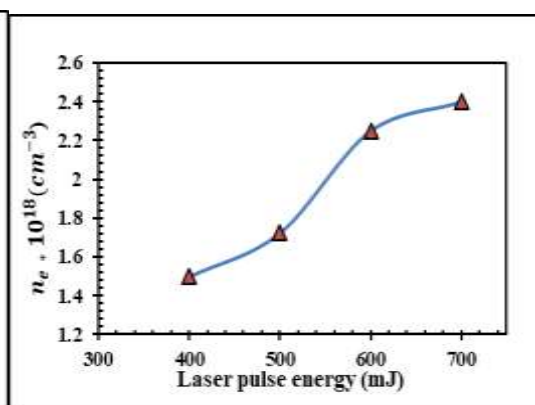**Figure 8:** Electron density of Pb plasm

Figure 9: Electron density of the S plasma

3.4 Determination of Debye Length

Debye length (λ_D) is a measure of the thickness of the sheath or shielding distance which can be calculated from[14]:

$$\lambda_D = \left(\frac{\varepsilon_o k_B T_e}{n_e^2}\right)^{\frac{1}{2}} \cong 743 \times \left(\frac{T_e \ (eV)}{n_e}\right)^{\frac{1}{2}} \qquad \ldots\ldots\ldots (3)$$

where: k_B is Boltzmann constant, ε_o is the permittivity of free space, e is the electron charge, T_e is the electron temperature, and n_e is electron density. The values of Debye length for lead and sulfur plasma were studied as a function of laser energy, as shown in Table 1 and Figure 10 for lead and Table 2 and Figure 11 for sulfur. These results agree with those of Aadim [15].
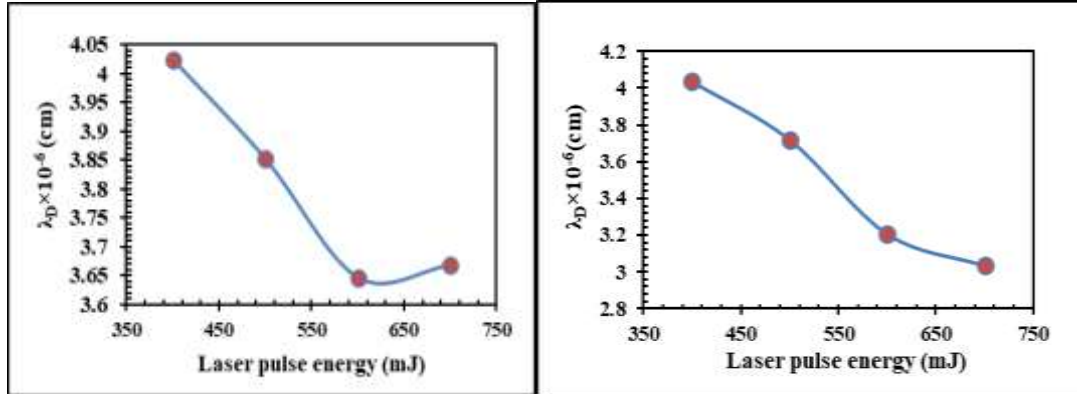

Figure 10: Debye length of the Pb plasma **Figure 11:** Debye length of the S plasma

3.5 Determination of Plasma Frequency

The quantity ω_p called the plasma frequency can be calculated [14]:

$$\omega_p = \sqrt{\frac{e^2 n_e}{m_e \varepsilon_o}} \qquad \ldots\ldots\ldots(4)$$

Where: e is the electron charge, ε_o is the permittivity of free space, n_e is the electron density and m_e is the mass of the electron. The change of the plasma frequency with laser energy is shown in Figure 12 for lead plasma and Figure 13 for sulfur plasma. With increasing laser pulse energies, the plasma frequency rises, which is due to an increase in electron concentration as a result of an inverse Bremsstrahlung process leading to an increase in frequency, as shown in Table 1 for Pb and Table 2 for S. These results agree with those of Aadim [15].
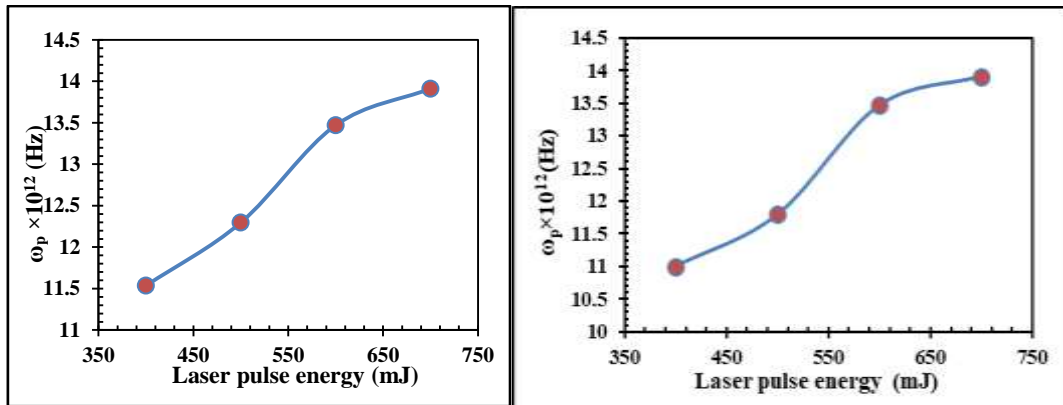

Figure 12: Plasma frequency of the Pb plasma **Figure 13:** Plasma frequency of the S plasma

Table 1: Plasma parameters for Pb plasma with different laser pulse energy

E(mJ)	FWHM (nm)	$n_e \times 10^{18}$ (cm^{-3})	$\lambda_D \times 10^{-6}$ (cm)	T_e(eV)	$\omega_p \times 10^{12}$ (Hz)	N_d
400	2.20	1.65	4.02	0.48	11.53	449
500	2.50	1.88	3.85	0.50	12.29	448
600	3.00	2.25	3.64	0.54	13.47	456
700	3.20	2.40	3.66	0.58	13.91	495

Table 2: Plasma parameters for S plasma with different laser pulse energy

E(mJ)	FWHM (nm)	$n_e \times 10^{18}$ (cm^{-3})	$\lambda_D \times 10^{-6}$ (cm)	T_e(eV)	$\omega_p \times 10^{12}$ (Hz)	N_d
400	2.00	1.50	4.03	0.44	10.99	413
500	2.30	1.73	3.72	0.43	11.79	372
600	3.00	2.25	3.20	0.42	13.47	311
700	3.20	2.40	3.03	0.40	13.91	281

4. Conclusions

As part of the current study, the optical emission spectroscopy method was used to investigate the effect of different laser energies (400-700 mJ) on the properties of the plasma and the emission spectra of lead and sulfur plasmas in order to better understanding of their interactions. The results revealed that the emission spectrum of the lead plasma falls within a range of 200 nm to 570 nm . The sulfur plasma has a wavelength range of 250 nm to 1100 nm. The parameters of the plasma can be determined through these emissions, the most important of which is temperature, which increased with the increase in laser energies in lead plasma from(0.48-0.58 eV). In contrast, it decreased for the sulfur plasma (0.44 - 0.40 eV). The electron density increased in lead plasma from 1.65×10^{18} to 2.4×10^{18} cm^{-3} , and it increased in the sulfur plasma between (1.5×10^{18}-2.4×10^{18} cm^{-3}). In addition, the Debye length and the frequency of the plasma were determined.

Acknowledgements

5. References

[1] D. W. Hahn and N. Omenetto, "Laser-induced breakdown spectroscopy (LIBS), part II: review of instrumental and methodological approaches to material analysis and applications to different fields," *Appl. Spectrosc.*, vol. 66, no. 4, pp. 347–419, 2012.

[2] H. K. Sanghapi, K. K. Ayyalasomayajula, F. Y. Yueh, J. P. Singh, D. L. McIntyre, J. C. Jain, J. Nakano, "Analysis of slags using laser-induced breakdown spectroscopy," *Spectrochim. Acta Part B: At. Spectrosc.*, vol. 115, pp. 40–45, 2016.

[3] A. A. Shaltout, N. Y. Mostafa, M. S. Abdel-Aal, and H. A. Shaban, "Electron number density and temperature measurements in laser produced brass plasma," *Eur. Phys. Journal-Applied Phys.*, vol. 50, no. 1, p. 11003, 2010.

[4] D. M. Wong, A. A. Bol'shakov, and R. E. Russo, "Laser induced breakdown spectroscopy," in *Encyclopedia of Spectroscopy and Spectrometry*, 2010, pp. 1281–1287.

[5] A. Iftikhar, Y. Jamil, N. Nazeer, M. S. Tahir, and N. Amin, "Optical Emission Spectroscopy of Nickel-Substituted Cobalt–Zinc Ferrite," *J. Supercond. Nov. Magn.*, vol. 34, no. 7, pp. 1849–1854, 2021, doi: 10.1007/s10948-020-05734-5.

[6] N. M. Shaikh, M. S. Kalhoro, A. Hussain, and M. A. Baig, "Spectroscopic study of a lead plasma produced by the 1064 nm, 532nm and 355 nm of a Nd:YAG laser," *Spectrochim. Acta - Part B: At. Spectrosc.*, vol. 88, pp. 198–202, 2013, doi: 10.1016/j.sab.2013.07.007.

[7] W. Zhang, R. Zhou, K. Liu, J. Yan, Q. Li, Z. Tang, X. Li, Q. Zeng, X. Zeng, "Sulfur determination in laser-induced breakdown spectroscopy combined with resonance Raman scattering," *Talanta*, vol. 216, p. 120968, 2020, doi: 10.1016/j.talanta.2020.120968.

[8] M. Fikry, W. Tawfik, and M. M. Omar, "Investigation on the effects of laser parameters on the plasma profile of copper using picosecond laser induced plasma spectroscopy," *Opt. Quantum Electron.*, vol. 52, no. 5, article no.: 249, 2020, doi: 10.1007/s11082-020-02381-x.

[9] Q. A. Abbas, "Effect of Target properties on the Plasma Characteristics that produced by Laser at Atmospheric Pressure," *Iraqi J. Sci.*, vol. 60, no. 6, pp. 1251–1258, 2019.

[10] M. Hanif, M. Salik, and M. A. Baig, "Diagnostic study of nickel plasma produced by fundamental (1064 nm) and second harmonics (532 nm) of an Nd: YAG laser," *J. Mod. Phys.*, vol. 3, no. 10A, p. 1663, 2012.

[11] M. Hanif, M. Salik, and M. A. Baig, "Spectroscopic studies of the laser produced lead plasma," *Plasma Sci. Technol.*, vol. 13, no. 2, pp. 129–134, 2011, doi: 10.1088/1009-0630/13/2/01.

[12] M. Hanif, M. Salik, and M. A. Baig, "Quantitative studies of copper plasma using laser induced breakdown spectroscopy," *Opt. Lasers Eng.*, vol. 49, no. 12, pp. 1456–1461, 2011, doi: 10.1016/j.optlaseng.2011.06.013.

[13] R. Mohammed, K. Aadim, and K. Ahmed, "Laser Intensity and Matrix Effect on Plasma Parameters for CuZn, Cu, and Zn Produced by Nd:YAG Laser," *Acta Phys. Pol. A*, vol. 140, no. 4, pp. 306–310, 2021, doi: 10.12693/aphyspola.140.306.

[14] F. F. Chen, "Erratum to: Introduction to Plasma Physics and Controlled Fusion," in *Introduction to Plasma Physics and Controlled Fusion*, Springer, 2018, pp. E1–E1.

[15] K. A. Aadim, "Characterization of Laser induced cadmium plasma in air," *Iraqi J. Sci.*, vol. 56, no. 3B, pp. 2292–2296, 2015.